THE JOURNAL OF BIOLOGICAL CHEMISTRY VOL. 288, NO. 10, pp. 7169–7181, March 8, 2013

β-Arrestin Recruitment and G Protein Signaling by the Atypical Human Chemokine Decoy Receptor CCX-CKR*

Received for publication, July 30, 2012, and in revised form, November 23, 2012 Published, JBC Papers in Press, January 22, 2013, DOI 10.1074/jbc.M112.406108

Anne O. Watts[‡1], Folkert Verkaar[‡§1], Miranda M. C. van der Lee[§], Claudia A. W. Timmerman[§], Martien Kuijer[‡], Jody van Offenbeek[‡§], Lambertus H. C. J. van Lith[§], Martine J. Smit[‡], Rob Leurs[‡], Guido J. R. Zaman[¶], and Henry F. Vischer[‡2]

From the [‡]Division of Medicinal Chemistry, Faculty of Sciences, VU University Amsterdam, 1081 HV Amsterdam, The Netherlands, the [§]Merck Research Laboratories, Molecular Pharmacology & DMPK, 5340 BH Oss, The Netherlands, and the [¶]Netherlands Translational Research Center B.V., 5340 AG Oss, The Netherlands

Background: CCX-CKR is considered to be a chemokine decoy receptor that is unable to signal.
Results: Chemokines induce β-arrestin recruitment to CCX-CKR and pertussis toxin (PTX)-dependent CRE activity.
Conclusion: PTX-sensitive G proteins hinder CCX-CKR coupling to other G proteins and consequently keep receptors silent.
Significance: Recruitment of β-arrestin to CCX-CKR requests re-evaluation of the signaling capacity of this atypical receptor.

Chemokine receptors form a large subfamily of G protein-coupled receptors that predominantly activate heterotrimeric G_i proteins and are involved in immune cell migration. CCX-CKR is an atypical chemokine receptor with high affinity for CCL19, CCL21, and CCL25 chemokines, but is not known to activate intracellular signaling pathways. However, CCX-CKR acts as decoy receptor and efficiently internalizes these chemokines, thereby preventing their interaction with other chemokine receptors, like CCR7 and CCR9. Internalization of fluorescently labeled CCL19 correlated with β-arrestin2-GFP translocation. Moreover, recruitment of β-arrestins to CCX-CKR in response to CCL19, CCL21, and CCL25 was demonstrated using enzyme-fragment complementation and bioluminescence resonance energy transfer methods. To unravel why CCX-CKR is unable to activate G_i signaling, CCX-CKR chimeras were constructed by substituting its intracellular loops with the corresponding CCR7 or CCR9 domains. The signaling properties of chimeric CCX-CKR receptors were characterized using a cAMP-responsive element (CRE)-driven reporter gene assay. Unexpectedly, wild type CCX-CKR and a subset of the chimeras induced an increase in CRE activity in response to CCL19, CCL21, and CCL25 in the presence of the G_i inhibitor pertussis toxin. CCX-CKR signaling to CRE required an intact DRY motif. These data suggest that inactive G_i proteins impair CCX-CKR signaling most likely by hindering the interaction of this receptor with pertussis toxin-insensitive G proteins that transduce signaling to CRE. On the other hand, recruitment of the putative signaling scaffold β-arrestin to CCX-CKR in response to chemokines might allow activation of yet to be identified signal transduction pathways.

Chemokine receptors form a large family of G protein-coupled receptors (GPCRs)[3] involved in migration, activation, and differentiation of immune cells. The 19 known human chemokine receptors and their ~50 endogenous peptide ligands form a complex system in which many chemokine receptors can bind multiple chemokines, and many chemokines can bind more than one receptor (1). Chemokine receptors signal predominantly via heterotrimeric G_i proteins, resulting in an inhibition of cAMP production by adenylyl cyclases and induction of intracellular calcium mobilization (2). Interestingly, the chemokine receptors D6, DARC, CCX-CKR, CXCR7, and CCRL2 bind chemokines with high affinity, but ligand binding does not result in G protein-mediated intracellular calcium mobilization or chemotaxis (3). Rather, these atypical chemokine receptors act as decoy receptors to regulate chemokine availability. Upon internalization, the receptor-bound chemokines are either targeted for lysosomal degradation or transported across the cell to be subsequently exposed or released on the other side of the cell (*i.e.* transcytosis) (3). CCX-CKR is a high affinity receptor for the chemokines CCL19/ELC, CCL21/SLC, and CCL25/TECK (4). These chemokines are important for the development of acquired immunity by activating CCR7 or CCR9. CCL19 and CCL21 recruit CCR7-expressing dendritic and T cells into the T cell compartments of secondary lymphoid organs (5). CCL25, on the other hand, recruits antigen-experienced lymphocytes to the small intestine by activating CCR9 (6). Mouse CCX-CKR knock-out models demonstrated that CCX-CKR is important for steady-state homing of dendritic cells to skin-draining lymph nodes, T cell differentiation, and immune response kinetics in an experimental autoimmune encephalomyelitis model, by regulating local chemokine levels (7, 8). Moreover, CCR7 and CCR9 have been shown to play a role in various cancers (9). CCX-CKR scavenges CCL19 and CCL21 both *in vitro* and *in vivo*, thereby decreasing

* This work was supported by the Dutch Top Institute Pharma initiative program D1–105.
[1] These authors contributed equally to this work.
[2] To whom correspondence should be addressed: VU University Amsterdam, De Boelelaan 1083, 1081 HV Amsterdam, The Netherlands. E-mail: h.f.vischer@vu.nl.

[3] The abbreviations used are: GPCR, G protein-coupled receptor; CRE, cAMP-responsive element; ERK1/2, extracellular stimulus-regulated kinase 1/2; PTX, pertussis toxin; Rluc, *Renilla* luciferase; TM, transmembrane; PTH1R, parathyroid hormone receptor 1; EA, enzyme acceptor; BRET, bioluminescence resonance energy transfer; FSK, forskolin; IL, intracellular loop.

the free concentration of these chemokines (7, 8, 10). Indeed, low CCX-CKR expression levels in breast cancer tumor cells were correlated with an increase in lymph node metastasis and consequently poor survival rate of patients (11). Additionally, CCX-CKR has been suggested to mediate CCL19 and CCL21 transcytosis across lymphatic endothelium, although direct evidence is still lacking (12). CCX-CKR is expressed in many tissues, including heart, lung, and intestine, as well as by stromal cells of skin-draining lymph nodes, thymic epithelial cells, and a number of hematopoietic cell types (4, 7, 8, 13–16). Transgenic overexpression of CCX-CKR decreased hematopoietic precursor cell numbers in the thymic anlage at embryonic stages, whereas cell numbers returned to normal levels in newborn and adult mice (7).

Following or alternative to G protein coupling, activated GPCRs can also recruit β-arrestin upon phosphorylation of their intracellular domains. β-Arrestin bound to the GPCR may then act as a scaffold protein for receptor internalization and G protein-independent signaling to, for example, extracellular stimulus-regulated kinase 1/2 (ERK1/2) and Akt (protein kinase B) (17). The atypical chemokine receptor CXCR7 is internalized and signals exclusively through β-arrestin in a chemokine-dependent manner (18, 19). D6 constitutively recruits β-arrestin, which is essential for the observed continuous internalization of D6 (20). However, a more recent study provided evidence that β-arrestin was not necessarily involved in D6 internalization but increased receptor stability (21). CCX-CKR has been previously suggested to internalize CCL19 in a β-arrestin-independent manner (10). In the present study, however, we demonstrate for the first time the concentration-dependent recruitment of β-arrestins to the atypical chemokine receptor CCX-CKR upon stimulation with CCL19, CCL21, or CCL25 using three different methodologies in various transfected cell lines. Moreover, we provide evidence that G_i proteins impair CCX-CKR-mediated signaling to CRE. These new aspects of CCX-CKR signaling provide additional avenues through which the role of CCX-CKR may be further explored.

EXPERIMENTAL PROCEDURES

Materials—Cell culture media were purchased from PAA Laboratories GmbH (Pasching, Austria). All nonlabeled chemokines were obtained from PeproTech (London, UK). Alexa Fluor 647-labeled CCL19 (CCL19-AF) was purchased from Almac (Craigavon, UK). ^{125}I-Labeled CCL19 (^{125}I-CCL19) was purchased from PerkinElmer Life Sciences. Parathyroid hormone (PTH1–34) was obtained from Bachem (Bubendorf, Switzerland). Anti-mouse IgG-Alexa Fluor 647 and anti-rat IgG-Alexa Fluor 647 were purchased from R&D Systems. Unless stated otherwise, all chemicals were purchased from Sigma. Nonidet P-40 was purchased from Roche Diagnostics.

DNA Constructs—pCMV-Prolink was purchased from DiscoveRx (Fremont, CA). Full-length human CCX-CKR in pECFP-N1 was provided by Marloes van der Zwam (Universitair Medisch Centrum Groningen, Groningen, The Netherlands). KOZAK-optimized CCX-CKR cDNA was amplified from this vector using PCR with Phusion polymerase enzyme (Finnzymes, Espoo, Finland) and was subcloned into pCMV-Prolink. cDNA encoding the CCX-CKR extended at the N terminus with 3 HA tags (HA_3-CCX-CKR) and pertussis toxin (PTX)-insensitive mutants of $G\alpha_{i1}$, $G\alpha_{i2}$, and $G\alpha_{i3}$ ($G\alpha_i$/C351I), each in pcDNA3.1$^+$ (Invitrogen), were purchased from Missouri S&T cDNA Resource Center (Rolla, MO). cDNA encoding CCX-CKR in pcDNA3.1 was a gift from Dr. Biber (Universitair Medisch Centrum Groningen, Groningen, The Netherlands). CCX-CKR and HA_3-CCX-CKR were subcloned into pcDEF3 (a gift from Dr. Langer, Robert Wood Johnson Medical School, Piscataway, NJ). CCX-CKR cDNA was fused in-frame with *Renilla* luciferase (Rluc) using a PCR-based method, as previously described (22). β-Arrestin1 and β-arrestin2 enhanced yellow fluorescent protein EYFP fusion constructs were described previously (23). The R3.50A mutant of CCX-CKR was constructed by site-directed mutagenesis and re-introduced into pcDEF3 (CCX/R3.50A). To construct the other CCX-CKR mutants, unique restriction endonuclease sites were first introduced by synthesizing a CCX-CKR-encoding DNA fragment (GenScript, Piscataway, NJ) with the following silent mutations: ^{399}CAGCAT^{404} into ^{399}ATCGAT^{404} to introduce ClaI in transmembrane (TM) helix 3-encoding sequence, ^{600}TCAAATGCTAG^{610} into ^{600}CCAAATGCTGG^{610} to introduce PflmI in TM5, ^{858}AGTCACA^{864} into ^{858}GGTCACC^{864} to introduce BstEII in TM7, and ^{922}GCATCT^{927} into ^{922}GCTAGC^{927} to introduce NheI in intracellular helix 8. This synthesized fragment was subcloned in pcDEF3 using BamHI and XbaI sites that flanked the open reading frame at the 5′- and 3′-end. Next, synthesized DNA sequences coding for IL2 and IL3 loops of CCR7 or CCR9 were inserted using ClaI-BlpI and PflmI-BstEII, respectively (Fig. 5). The C-terminal S(T/A)-encoding DNA fragment was introduced using NheI-XbaI. All generated constructs were sequence verified prior to use.

The human parathyroid hormone receptor 1 (PTH1R) cDNA was provided by Winfried Mulder (Merck Research Laboratories, Oss, The Netherlands) and subsequently subcloned into pIRESpuro2 (Clontech, Mountain View, CA). Bioluminescence resonance energy transfer (BRET)-based cAMP biosensor (pcDNA3.1-(L)-His-CAMYEL, number ATCC-MBA-277) was purchased from American Type Culture Collection (Manassas, VA) (24).

Cell Culture and Transfection—All cells were maintained at 37 °C in a humidified atmosphere containing 5% CO_2. U2OS cells stably expressing green fluorescent protein (GFP)-tagged human β-arrestin2 (U2OS-β-arr2-GFP) were described previously (25). U2OS-β-arr2-GFP cells were stably transfected with pcDEF3-HA_3-CCX-CKR and pIRESpuro2 in a 4:1 molar ratio using FuGENE 6 transfection reagent (Roche Diagnostics), followed by selection of single cell clones by addition of 2 μg/ml of puromycin (Calbiochem, San Diego, CA) to culture medium. The U2OS-PTH1R cell line was derived from U2OS-β-arr2-GFP by transfection of pIRESpuro2-PTH1R and selection with 2 μg/ml of puromycin.

Parental Chinese hamster ovary (CHO)-K1 PathHunter cells stably expressing β-arrestin2 coupled to an inactive N-terminal β-galactosidase deletion mutant termed enzyme acceptor (β-arrestin2-EA) were purchased from DiscoveRx (Fremont,

CA), and are referred to in this paper as CHO-β-arr2 cells. These cells were maintained in DMEM/F-12 supplemented with 10% (v/v) bovine calf serum (Hyclone, Logan, UT), 250 μg/ml of hygromycin, 100 units/ml of penicillin, and 100 μg/ml of streptomycin (all from Invitrogen). CHO-β-arr2 cells were stably transfected with pCMV-CCX-CKR-Prolink using Lipofectamine 2000 (Invitrogen) to yield the CHO-CCX-CKR cell line. CHO-K1 PathHunter cells stably expressing PTH1R-ProLink, CCR7-ProLink, and CCR9-ProLink (CHO-PTH1R, CHO-CCR7, CHO-CCR9, respectively) were purchased from DiscoveRx, and cultured in the medium mentioned above, supplemented with 800 μg/ml of geneticin (Invitrogen). HEK293T cells were purchased from American Type Culture Collection (ATCC) and maintained in DMEM supplemented with 10% (v/v) fetal calf serum (Integro, Dieren, The Netherlands), 50 IU/ml of penicillin, and 50 μg/ml of streptomycin. For radioligand binding, ELISA, and reporter gene assays, HEK293T cells were transiently co-transfected with 500 ng/1 × 10^6 cells CRE-Luc DNA, 125 ng/1 × 10^6 cells receptor DNA in the absence or presence of 63 ng/1 × 10^6 cells Gα subunit DNA using linear polyethylenimine (MW 25,000; Polysciences, Warrington, PA) as described previously (26). For BRET-based β-arrestin1/2 recruitment assays, the HEK293T cells were co-transfected with 250 ng of CCX-CKR-Rluc and 1 μg of β-arrestin1/2-EYFP DNA per 1 × 10^6 cells, whereas 125 ng of CCX-CKR cDNA was co-transfected with 250 ng of pcDNA3.1-(L)-His-CAMYEL for the BRET-based cAMP biosensor experiments.

High Content Analysis of β-Arrestin-2 Redistribution—U2OS-β-arr2-GFP, U2OS-PTHR1, or U2OS-CCX-CKR cells were seeded in clear-bottom 96-well plates (PerkinElmer Life Sciences) with 15,000 cells/well in 90 μl of assay medium (DMEM/F-12 supplemented with 2% (v/v) fetal calf serum, 100 units/ml of penicillin, and 100 μg/ml of streptomycin) and cultured overnight. The following day, medium was replaced with 45 μl of assay medium. Five microliters of assay medium containing chemokines was added and cells were incubated at 37 °C for 45 min. Cells were fixed in 4% (v/v) paraformaldehyde (BioConnect, Huissen, The Netherlands) and incubated with 1 μM Hoechst (Invitrogen) in PBS for 30 min. Plates were analyzed on an Operetta automated fluorescence microscope (PerkinElmer Life Sciences).

Enzyme Fragment Complementation-based β-Arrestin Recruitment Assays—Cells were seeded in 384-well CulturPlates (PerkinElmer) at 10,000 cells/well in 15 μl of Opti-MEM (Invitrogen) containing 1% (v/v) bovine calf serum (assay medium). The next day, cells were stimulated with 10 μl of chemokine in assay medium and then returned to the incubator for 90 min. Cells were disrupted using 12 μl of substrate-containing lysis buffer from the PathHunter Detection Kit in the formulation specified by the supplier (DiscoveRx). Plates were incubated in the dark for 90 min at room temperature before measurement of β-galactosidase activity (luminescence) on an Envision multilabel plate reader (PerkinElmer).

BRET-based β-Arrestin Recruitment Assay—One day after transfection, HEK293T cells were transferred to poly-L-lysine-coated white 96-well plates. Growth medium contained 100 ng/ml of PTX (Sigma) where applicable. The next day, medium was replaced with Hanks' balanced salt solution containing 100 ng/ml of PTX where applicable and fluorescence was measured on a Victor^3 multilabel plate reader (excitation 485 nm; emission 535 nm; PerkinElmer Life Sciences). Ten minutes after addition of coelenterazine-h (5 μM final concentration; Promega, Madison, WI), ligand solutions in Hanks' balanced salt solution supplemented with 0.05% BSA were added in the stated concentrations and incubated for an additional 5 min. BRET (emission 535 nm) and Rluc expression (emission 460 nm) were measured with a Victor^3 multilabel plate reader. Baseline-corrected BRET ratios were calculated by first dividing BRET by Rluc emission values, followed by subtraction of the BRET ratio of cells expressing CCX-CKR-Rluc alone.

cAMP Accumulation Assay— cAMP measurements in CHO-CCX-CKR cells were performed with a homogenous time-resolved fluorescence kit from Cisbio (Gif-sur-Yvette, France) essentially as described previously (27). Briefly, chemokines diluted in 10 μl of dilution buffer either containing forskolin (0.5 μM final concentration) or DMSO control were dispensed in 384-well OptiPlates (PerkinElmer Life Sciences). Subsequently, 7,500 CHO-CCX-CKR cells in 10 μl of assay medium (DMEM/F-12 containing 5 μg/ml of apo-transferrin (Sigma), 1 μg/ml of insulin, 100 units/ml of penicillin, and 100 μg/ml of streptomycin) were added and plates were incubated at 37 °C for 60 min. Cells were disrupted by addition of 10 μl of cAMP-XL665 conjugate and 10 μl of Europium-labeled anti-cAMP antibody diluted in lysis buffer (all provided with the kit). Plates were incubated in the dark at room temperature for 60 min before measurement of time-resolved fluorescence at 615 and 665 nm on an Envision multilabel plate reader (PerkinElmer Life Sciences). Absolute cAMP concentrations were calculated from a cAMP standard.

Inositol Phosphate Accumulation Assay—Inositol phosphate measurements in CHO-CCX-CKR cells were performed using a homogenous time-resolved fluorescence kit from Cisbio (Gif-sur-Yvette, France). CHO-CCX-CKR cells were plated in 384-well proxiPlates with 10,000 cells/well in 20 μl of assay medium (DMEM/F-12 containing 10% (v/v) fetal calf serum, 100 units/ml of penicillin, and 100 μg/ml of streptomycin) and were allowed to adhere overnight. Medium was aspirated and cells were stimulated with 14 μl of chemokine in stimulation buffer (provided in the kit) containing 0.1% (w/v) bovine serum albumin (BSA; Sigma). Plates were incubated at 37 °C for 90 min before the addition of 3 μl of IPone-XL665 conjugate and 3 μl of Europium-labeled anti-IPone antibody diluted in lysis buffer (all provided with the kit). Plates were incubated in the dark at room temperature for 60 min before measurement of time-resolved fluorescence at 615 and 665 nm on an Envision multilabel plate reader. Absolute IPone concentrations were calculated from an IPone standard.

Western Blotting—Isolation of CHO-CCX-CKR lysates and Western blotting was performed as described previously (25). The following antibodies were used at the indicated dilutions: mouse anti-β-actin, 1:5000 (Abcam, Cambridge, UK); rabbit anti-total Akt, 1:1000; rabbit anti-phospho-Ser^{473}; Akt, 1:1000; rabbit anti-phospho-Thr^{202}/Tyr^{204} ERK1/2, 1:2000 (Cell Signaling Technology, Danvers, MA); mouse anti-total ERK1/2, 1:2000 (Invitrogen); anti-mouse HRP conjugate, 1:2000; and anti-rabbit HRP conjugate, 1:2000 (Promega).

TABLE 1

CCL19, CCL21, and CCL25 affinities and β-arrestin recruitment potencies at CCX-CKR

pK_i values of ^{125}I-CCL19 displacement by CCL19, CCL21, and CCL25 and pEC_{50} values to recruit β-arrestin are given as averages ± S.E. Number of independent experiments that were performed in triplicate are indicated in parentheses.

	Binding	β-Arrestin2-GFP translocation	β-Arrestin2 EFC	β-Arrestin2 BRET	β-Arrestin1 BRET
	pK_i		pEC_{50}		
CCL19	8.4 ± 0.5 (2)	8.5 ± 0.2 (5)	8.9 ± 0.2 (6)	9.1 ± 0.1 (3)	9.1 ± 0.1 (3)
CCL21	6.9 ± 0.4 (2)	7.9 ± 0.1 (5)	8.0 ± 0.1 (4)	8.5 ± 0.1 (3)	8.5 ± 0.2 (4)
CCL25	7.6 ± 0.1 (2)	7.9 ± 0.1 (5)	7.8 ± 0.1 (4)	8.1 ± 0.1 (2)	8.3 ± 0.1 (2)

Cyclic AMP-responsive Element (CRE)-driven Reporter Gene—One day after transfection, HEK293T cells were transferred to poly-L-lysine-coated white 96-well plates. Where required, growth medium contained 100 ng/ml of PTX. The following day, growth medium was replaced with serum-free medium supplemented with 0.05% BSA and 100 ng/ml of PTX, 1 μM forskolin (FSK), and/or ligands, as indicated. After 6 to 8 h incubation at 37 °C, stimulation medium was removed and cells were incubated for 5 min with 25 μl of substrate solution (39 mM Tris·H_3PO_4, pH 7.8, 39% glycerol, 2.6% Triton X-100, 860 μM dithiothreitol, 18 mM $MgCl_2$, 825 μM ATP, 77 μM disodium pyrophosphate, 230 μg/ml of beetle luciferin) (Promega). Luminescence was measured using a Victor^3 multilabel plate reader.

BRET-based cAMP Biosensor Assay—Changes in cAMP levels were detected using a BRET-based cAMP sensor in a similar manner as the BRET-based β-arrestin recruitment assay, except that cells were rinsed once with Hanks' balanced salt solution, and incubated with fresh Hanks' balanced salt solution for 30 min before being stimulated. In addition, the non-specific phosphodiesterase 3-isobutyl-1-methylxanthine was added simultaneously with coelenterazine-h to a final concentration of 40 μM (23).

Radioligand Binding and Internalization—One day after transfection, HEK293T cells were transferred to poly-L-lysine (Sigma)-coated 96-well plates. The next day, whole cells were incubated for 4 h at 4 °C with ~0.75 nM ^{125}I-CCL19 in binding buffer (50 mM HEPES, 100 mM NaCl, 1 mM $CaCl_2$, 5 mM $MgCl_2$, pH 7.4, 0.5% BSA) containing the indicated concentrations of unlabeled displacer. Incubations were terminated by washing the cells with ice-cold wash buffer (50 mM HEPES, 0.5 M NaCl, 1 mM $CaCl_2$, 5 mM $MgCl_2$, pH 7.4) followed by lysis in RIPA buffer (0.5% Nonidet P-40, 0.5% sodium deoxycholate, and 0.1% sodium dodecyl sulfate). Cell lysates were transferred to vials and counted in a Wallac Compugamma counter (PerkinElmer Life Sciences).

^{125}I-CCL19 internalization assays were performed in a similar manner as binding assays on intact cells, except that incubations were performed in a 37 °C waterbath (28). Incubations were terminated at the indicated time intervals by placing the 48-well plates on ice and rapid removal of free ^{125}I-CCL19 by washing the cells three times with ice-cold wash buffer. The fraction ^{125}I-CCL19 bound to receptors at the cell surface was removed using ice-cold acidified DMEM (pH 2.0). The cells were then solubilized in RIPA buffer to collect the acid-resistant (*i.e.* internalized) ^{125}I-CCL19 fraction, which was quantified using a Wallac Compugamma counter. Control experiments confirmed that acid treatment removed all surface-bound chemokine.

ELISA—One day after transfection, HEK293T cells were seeded in 96-well plates and cultured overnight. Next, the cells were fixed for 30 min with 4% formaldehyde in PBS and washed twice with Tris-buffered saline (TBS; 150 mM NaCl, 10 mM Tris·HCl, pH 7.5). Half of the samples were permeabilized by incubating the cells for 30 min with 0.5% Nonidet P-40 in TBS after fixation. Samples were then blocked for 4 h at room temperature with 1% fat-free milk in 0.1 M $NaHCO_3$ (pH 8.6). Samples were incubated overnight at 4 °C with the mouse anti-hCCX-CKR clone 2F11 (a kind gift from Dr. Chiba, Tokyo University of Science, Japan) diluted 1:1000 in TBS containing 1% fat-free milk powder and subsequently washed with TBS. Samples were incubated for 3 h at room temperature with goat anti-mouse HRP-conjugated antibody (Bio-Rad) diluted 1:2500 in 0.1 M $NaHCO_3$ (pH 8.6), containing 1% fat-free milk powder. After samples were washed with TBS, OPD substrate solution (2.2 mM *o*-phenylenediamine, 35 mM citric acid, 66 mM Na_2HPO_4, 0.015% H_2O_2, pH 5.6) was added. The reaction was stopped by addition of 1 M H_2SO_4 and the absorbance at 490 nm was measured with a PowerWave plate reader (BioTek, Winooski, VT).

Data Analysis—Sigmoidal concentration-response curves were plotted using GraphPad Prism 5.0 software. All data are presented as averages of mean ± S.E. Statistical analyses were performed using GraphPad Prism 5.0 software.

RESULTS

CCL19 Is Internalized by CCX-CKR and Co-localizes with β-Arrestin—CCX-CKR binds CCL19 with a ~6- and ~30-fold higher affinity (pK_i) than CCL25 and CCL21, respectively (Table 1). This rank order of binding affinities is in line with the previously reported 50% inhibitory concentration (IC_{50}) values (4). Hitherto, the only functional read-out for CCX-CKR has been the measurement of chemokine internalization (10). HEK293T cells transiently transfected with CCX-CKR internalized ^{125}I-CCL19 substantially faster than cells expressing CCR7 (Fig. 1*A*), which confirms previous observations (10). Next, CCX-CKR was stably expressed in U2OS human osteosarcoma cells that already express GFP-tagged β-arrestin2. These U2OS-CCX-CKR cells were treated for 45 min with 100 nM CCL19 conjugated to Alexa Fluor 647 (CCL19-AF) and imaged using automated high content fluorescence microscopy. CCL19-AF was internalized and accumulated in U2OS-CCX-CKR cells as indicated by the resistance to an acid wash (Fig. 1*B*, *panels 1* and *2*). Moreover, CCL19-AF internalization was impaired at 4 °C (Fig. 1*B*, *panels 3* and *4*). This accumulation of CCL19-AF in U2OS-CCX-CKR cells was CCX-CKR-dependent, as it was not observed when CCL19-AF was incubated with parental control cells (U2OS-β-arr2-GFP) or derived cells

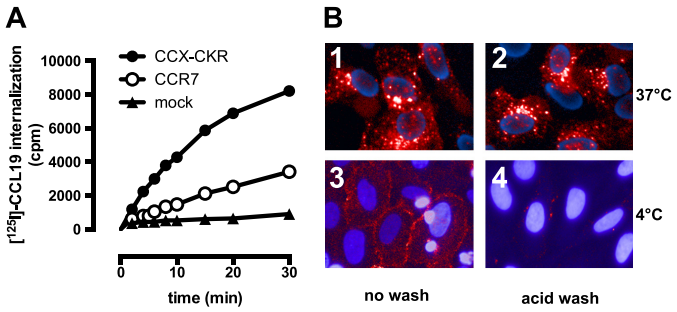

FIGURE 1. **CCX-CKR internalizes CCL19.** *A,* HEK293T cells transiently transfected with CCX-CKR, CCR7, or empty plasmid (*mock*) were incubated with ^{125}I-CCL19 for the indicated time. Surface bound ^{125}I-CCL19 was removed by an acid wash, and internalized ^{125}I-CCL19 was quantified. *B,* U2OS osteosarcoma cells expressing β-arrestin2 fused to green fluorescent protein (U2OS-β-arr2-GFP) were stably transfected with vector coding for CCX-CKR (U2OS-CCX-CKR cells). U2OS-CCX-CKR cells were treated with Alexa Fluor 647-coupled CCL19 (CCL19-AF) at 37 (*upper panels*) or 4 °C (*lower panels*) for 45 min. Then, cells were washed with an acidic buffer (0.2 M glycine (pH 3.0), 0.5 M NaCl) or PBS for 5 min before fixation and staining. Alexa Fluor 647 and Hoechst signals are depicted in *red* and *blue*, respectively.

that overexpressed the human parathyroid hormone receptor type 1 (U2OS-PTH1R) (data not shown). Next, it was evaluated whether chemokine binding to CCX-CKR can induce translocation of β-arrestin2-GFP to putative endocytic vesicles. In nonstimulated parental U2OS-β-arr2-GFP and U2OS-CCX-CKR cells, β-arrestin2-GFP was uniformly distributed throughout the cytoplasm (Fig. 2*A*, *panels 1* and *3*). In response to CCL19, β-arrestin2-GFP coalesced into vesicles in U2OS-CCX-CKR cells (Fig. 2*A*, *panel 4*). CCL19 was unable to cause β-arrestin2-GFP redistribution in parental U2OS-β-arr2-GFP cells that did not express CCX-CKR (Fig. 2*A*, *panel 2*) or in U2OS-β-arr2-GFP cells stably expressing PTH1R (U2OS-PTH1R) (data not shown). Subsequently, U2OS-CCX-CKR cells were treated with increasing concentrations of CCL19, CCL21, or CCL25 for 45 min and vesicle formation was quantified. The three chemokines had similar efficacy to induce β-arrestin2-GFP translocation (Fig. 2*B*), with CCL19 having a ~4-fold higher potency than CCL21 and CCL25 (Table 1). CCL19-AF induced β-arrestin2-GFP translocation with a similar potency as CCL19 (Fig. 2, *C*, *panels 1* and *4*, and *D*). Moreover, CCL19-AF co-localized with β-arrestin2-GFP in vesicles (Fig. 2*C*, *panels 4–6*). CCL19-AF induced β-arrestin2-GFP-vesicle and AF-vesicle formation with comparable potencies (Fig. 2*E*; Table 1).

The enzyme fragment complementation-based PathHunter™ β-arrestin assay was subsequently used to monitor enzyme acceptor-coupled β-arrestin2 (β-arr2-EA) recruitment to Prolink™-tagged CCX-CKR in response to chemokine stimulation. To this end, CCX-CKR-ProLink was stably expressed in CHO cells harboring β-arr2-EA (CHO-β-arr2). Stimulation of the resultant CHO-CCX-CKR cell line with CCL19, CCL21, and CCL25 for 90 min resulted in a concentration-dependent reconstitution of β-galactosidase enzyme activity as a consequence of the chemokine-induced close proximity between CCX-CKR-Prolink and β-arr2-EA (Fig. 3*A*). All three chemokines act as full agonists in recruiting β-arrestin2 to CCX-CKR in this enzyme fragment complementation-based assay format, with CCL19 being ~8- and ~12.5-fold more potent than CCL21 and CCL25, respectively (Table 1). As expected, CCL19 and CCL21 induced β-arr2-EA recruitment to CCR7-ProLink in CHO-CCR7 cells, whereas CCL25 stimulated the β-arr2-EA recruitment to CCR9-ProLink in CHO-CCR9 cells (data not shown). In contrast, the parental CHO-β-arr2 cells and those expressing the human parathyroid hormone receptor 1 (CHO-PTH1R) did not show an increase in β-galactosidase activity upon incubation with CCL19 (data not shown). Next, the potency and efficacy of a panel of chemokines to recruit β-arrestin2 to CCX-CKR in these CHO-CCX-CKR cells was evaluated. With the exception of CCL9/10, which acts as low potency (pEC_{50} = 6.2 ± 0.1) partial agonist (intrinsic activity $\alpha = 0.5$ in comparison to full agonist CCL19), all tested chemokines (*i.e.* vMIP-II, CCL3, CCL4, CCL6, CCL23, CXCL6, CXCL8, CXCL9, CXCL10, CXCL11, CXCL12, CXCL13) were unable to reconstitute β-galactosidase activity in these CHO-CCX-CKR cells when added up to a concentration of 1 μM (data not shown).

BRET technology was then used to confirm this close proximity between CCX-CKR and β-arrestin2 upon stimulation with CCL19, CCL21, and CCL25 (Fig. 3*B*; Table 1). Moreover, a similar concentration-dependent increase in BRET ratio was observed between CCX-CKR-Rluc and β-arrestin1-EFYP in response to these chemokines (Fig. 3*C*; Table 1). CCL19 was the most potent chemokine in inducing β-arrestin1/2 recruitment to CCX-CKR, whereas CCL21 and CCL25 had comparable potency. To evaluate whether β-arrestin1/2 recruitment to CCX-CKR required phosphorylation of the CCX-CKR C-terminal tail, all serine and threonine residues in this domain were alanine substituted (*i.e.* ^{323}SWRRQRQSVEEFPFDSEGPTEPTSTFS^{349} into ^{323}AWRRQRQAVEEFPFDAEGPAEPAAAFA^{349}). The expression level of this CCX-CKR-S(T/A)-Rluc mutant was ~60% of that of non-mutant CCX-CKR-Rluc, as determined by *Renilla* luciferase activity and ELISA on intact cells (data not shown). However, binding assays showed that CCX-CKR-S(T/A)-Rluc had no affinity for ^{125}I-CCL19 and ^{125}I-CCL25, and consequently was not able to recruit β-arrestin2-EYFP in response to chemokines (data not shown).

CCX-CKR Does Not Activate Typical Chemokine Receptor-induced β-Arrestin- or G Protein-mediated Signaling—To evaluate the ability of CCX-CKR to activate downstream effectors of β-arrestin signaling, CHO-CCX-CKR cells were stimulated with vehicle or 100 nM CCL19 for 2 to 90 min and lysates were probed for phosphorylation of ERK1/2 (Thr^{202}/Tyr^{204}) and Akt (Ser^{473}). CCL19-induced phosphorylation of ERK1/2 was not observed, whereas treatment with the positive reference PMA for 10 min elicited robust ERK1/2 phosphorylation (Fig. 4*A*). Furthermore, CCL19 did not affect Akt phosphorylation in CHO-CCX-CKR cells, whereas treatment with insulin caused a marked increase in Akt phosphorylation (Fig. 4*B*). In summary, no CCX-CKR-induced signaling to ERK1/2 or Akt was observed.

Because most chemokine receptors signal through G_i proteins upon receptor activation, CHO-CCX-CKR cells were stimulated with 100 nM CCL19, CCL21, or CCL25 for 60 min and cAMP levels were subsequently determined using an homogenous time-resolved fluorescence-based assay. These chemokines did not affect basal or FSK-induced cAMP accumulation, suggesting that CCX-CKR is not coupling to G_s or G_i

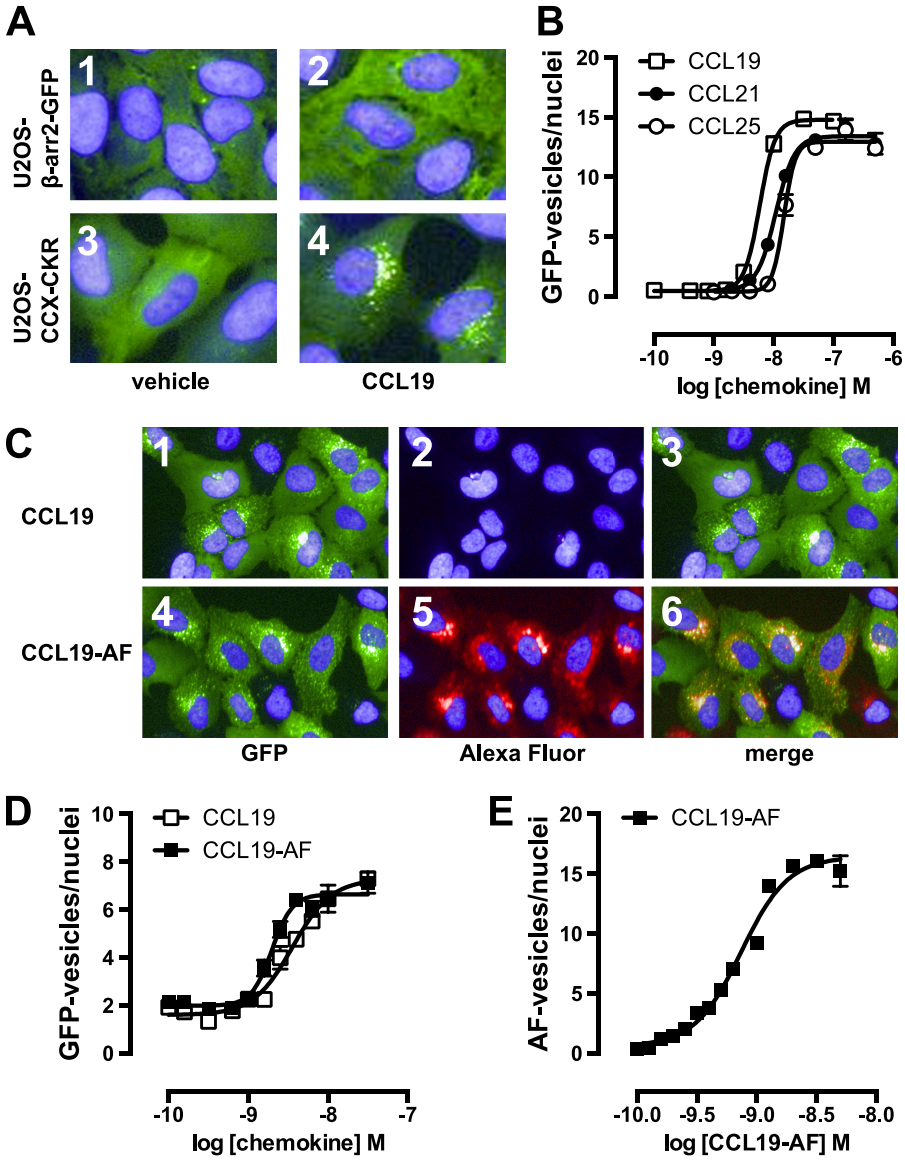

FIGURE 2. **Internalized CCL19 and β-arrestin co-localize in endocytic vesicles in cells expressing CCX-CKR.** *A*, U2OS-β-arr2-GFP and U2OS-CCX-CKR cells were treated with 100 nM CCL19 for 45 min. Cells were then fixed, stained with Hoechst, and imaged using fluorescence microscopy for GFP (*green*) and nuclei (*blue*). *B*, U2OS-CCX-CKR cells were stimulated with increasing concentrations of CCL19, CCL21, and CCL25 for 45 min. The recruitment of β-arrestin2 to CCX-CKR was quantified as the amount of GFP-containing vesicles per nucleus. *C*, U2OS-CCX-CKR cells were treated with 100 nM CCL19 or CCL19-AF for 45 min, followed by fluorescence microscopy. GFP is shown in *green*, Alexa Fluor 647 is in *red*, and nuclei are stained *blue*. *D*, U2OS-CCX-CKR cells were treated with increasing doses of CCL19 and CCL19-AF for 45 min followed by determination of GFP-containing vesicle formation. *E*, quantification of AF-containing vesicle formation of U2OS-CCX-CKR cells treated with increasing concentrations of CCL19-AF.

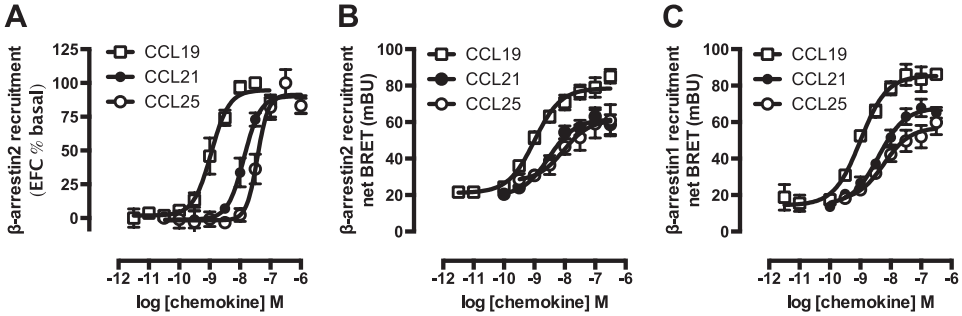

FIGURE 3. **CCX-CKR recruits β-arrestin1 and β-arrestin2 in a chemokine-dependent manner.** *A*, CHO cells stably expressing CCX-CKR fused to a peptide fragment of β-galactosidase and β-arrestin2 coupled to a complementary β-galactosidase mutant (CHO-CCX-CKR cells) were treated with ascending concentrations of CCL19, CCL21, and CCL25 for 90 min before measurement of β-galactosidase activity. *B* and *C*, potencies of β-arrestin2 (*B*) and β-arrestin1 (*C*) recruitment induced by CCL19 (*white squares*), CCL21 (*black circles*), and CCL25 (*white circles*) were determined using a BRET-based assay in HEK293T cells transiently co-transfected with CCX-CKR-Rluc and β-arrestin-EYFP. Data are presented as averages ± S.E. of 2–4 independent experiments performed in triplicate.

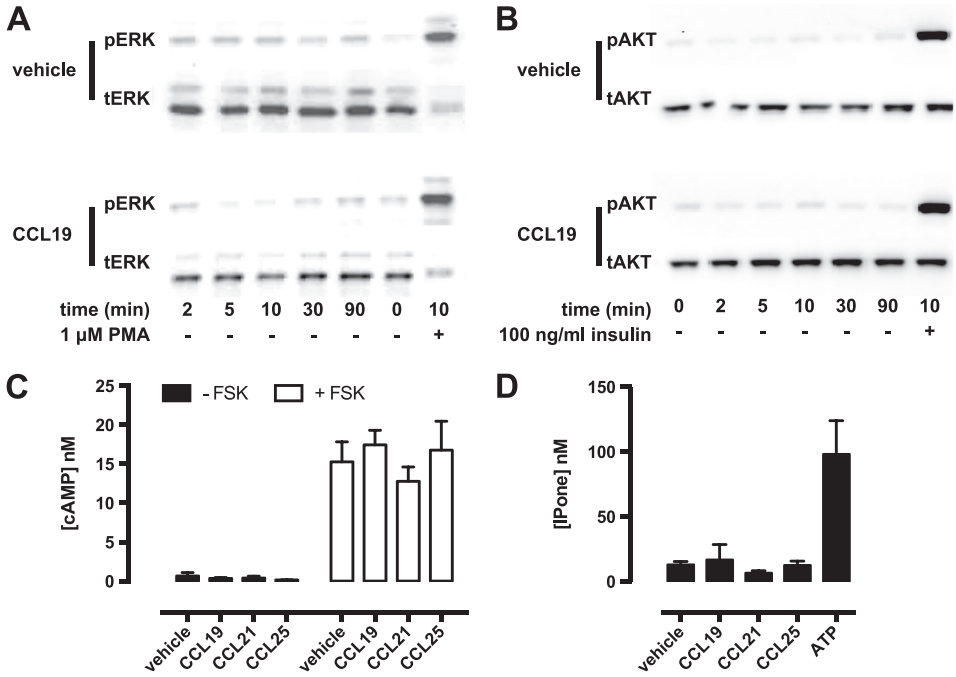

FIGURE 4. **CCX-CKR does not activate G protein-dependent or β-arrestin-dependent intracellular signaling pathways.** *A* and *B*, CHO-CCX-CKR cells were stimulated with 100 nM CCL19 or vehicle for several time periods. Control cells were treated with 1 μM PMA (*A*) or 100 ng/ml of insulin (*B*). Cell lysates were then analyzed for levels of (*A*) phosphorylated Thr^{202}/Tyr^{204}-ERK1/2 (*pERK*) and total ERK1/2 (tERK) or (*B*) phosphorylated Ser^{473}-Akt (*pAkt*) and total Akt (tAkt). *C*, CHO-CCX-CKR cells were treated with 100 nM CCL19, CCL21, and CCL25 in the presence or absence of 0.5 μM FSK for 60 min. Subsequently, cells were lysed and intracellular cAMP concentrations were measured. *D*, CHO-CCX-CKR cells were stimulated with 100 nM CCL19, CCL21, and CCL25 for 90 min before measurement of intracellular IPone concentrations. As a positive control, cells were treated with 100 μM ATP.

proteins, respectively (Fig. 4*C*). This was not due to an inability of the chemokines to induce such responses, as CCL19 and CCL25 decreased FSK-induced cAMP levels in CHO-CCR7 and CHO-CCR9 cells, respectively (data not shown). The ability of CCX-CKR to activate G_q proteins was also investigated. Intracellular inositol phosphate concentrations in CHO-CCX-CKR cells were not affected by treatment with CCL19, CCL21, and CCL25 (Fig. 4*D*). In contrast, inositol phosphate formation was observed in CHO-CCX-CKR cells after activation of endogenous purinoceptors by 100 μM ATP (Fig. 4*D*).

CCX-CKR IL2/3 Chimeras Stimulate cAMP Signaling—In contrast to CCR7 and CCR9, the atypical chemokine receptor CCX-CKR did not decrease FSK-induced cAMP levels in response to CCL19 and CCL25 stimulation. CCX-CKR chimeras were constructed by substitution of intracellular loop (IL) 2 and/or 3 with corresponding sequences of CCR7 and CCR9 to investigate whether intracellular domains of CCX-CKR might impede G protein coupling (Fig. 5*a*). These CCR7 and CCR9 ILs were hypothesized to confer G_i-coupling capacity to the CCX-CKR chimeras, resulting in decreased adenylyl cyclase activity. A CRE-driven luciferase reporter gene assay was used to quantify chemokine-stimulated changes in cAMP levels in HEK293T cells transiently expressing wild type CCX-CKR or CCX-CKR chimeras. Cell surface expression of all CCX-CKR chimeras was comparable ($p > 0.05$) to wild type CCX-CKR as measured by ELISA (Fig. 5*B*), whereas ^{125}I-CCL19 binding to CCX-CKR chimeras was significantly increased ($p < 0.05$) in comparison to wild type CCK-CKR (Fig. 5*C*). Except CCX/R9IL3 bound less ^{125}I-CCL19 than wild type CCX-CKR. As expected, FSK-induced CRE activity was decreased by treatment with 100 nM CCL19 in cells expressing CCR7 but not in cells transfected with wild type or chimeric CCX-CKR constructs (Fig. 5, *D* and *E*). CCL19 does not interact with CCR9 and consequently had no effect on FSK-induced CRE activity in CCR9-expressing cells. As a control for G_i-mediated signaling responses, cells were pre-treated overnight with 100 ng/ml of the inhibitor *Bordetella pertussis* toxin (PTX). As anticipated, PTX abolished the G_i-mediated decrease in CRE activity in CCR7-expressing HEK293T cells in response to CCL19. On the other hand, PTX significantly potentiated the CCL19-induced increase in CRE activity in cells expressing wild type CCX-CKR, CCX/R7IL3, CCX/R7IL2IL3, and CCX/R9IL2IL3 (Fig. 5*D*). Pre-treatment with PTX did not affect the binding affinities of CCL19, CCL21, and CCL25 for CCX-CKR (Fig. 6, *A–C*). Likewise, the potencies of these chemokines to recruit β-arrestin1/2 to CCX-CKR were not affected by PTX (Fig. 6, *D–I*). Next, the effect of CCL19 treatment on basal adenylyl cyclase activity was measured in the absence and presence of PTX pre-treatment. Only cells expressing CCX/R9IL2 showed a significant increase in CRE activity upon stimulation with CCL19 in the absence of FSK and PTX as compared with vehicle-treated cells (Fig. 5*E*). Interestingly, PTX pre-treatment increased CCL19-induced CRE activity in cells expressing wild type CCX-CKR, CCX/R7IL2, CCX/R7IL2IL3, and CCX/R9IL2IL3 (Fig. 5*E*). The absence of CCL19 responsiveness of CCX/R9IL3 with and without PTX pre-treatment might be related to the reduction in CCL19 binding to this mutant receptor as compared with wild type CCX-CKR (Fig. 5*C*). The CCR9 chemokine CCL25 showed a comparable CRE-inducing activity profile on CCX-CKR and CCX-CKR chimeras as CCL19 (Fig. 5, *F* and *G*). As

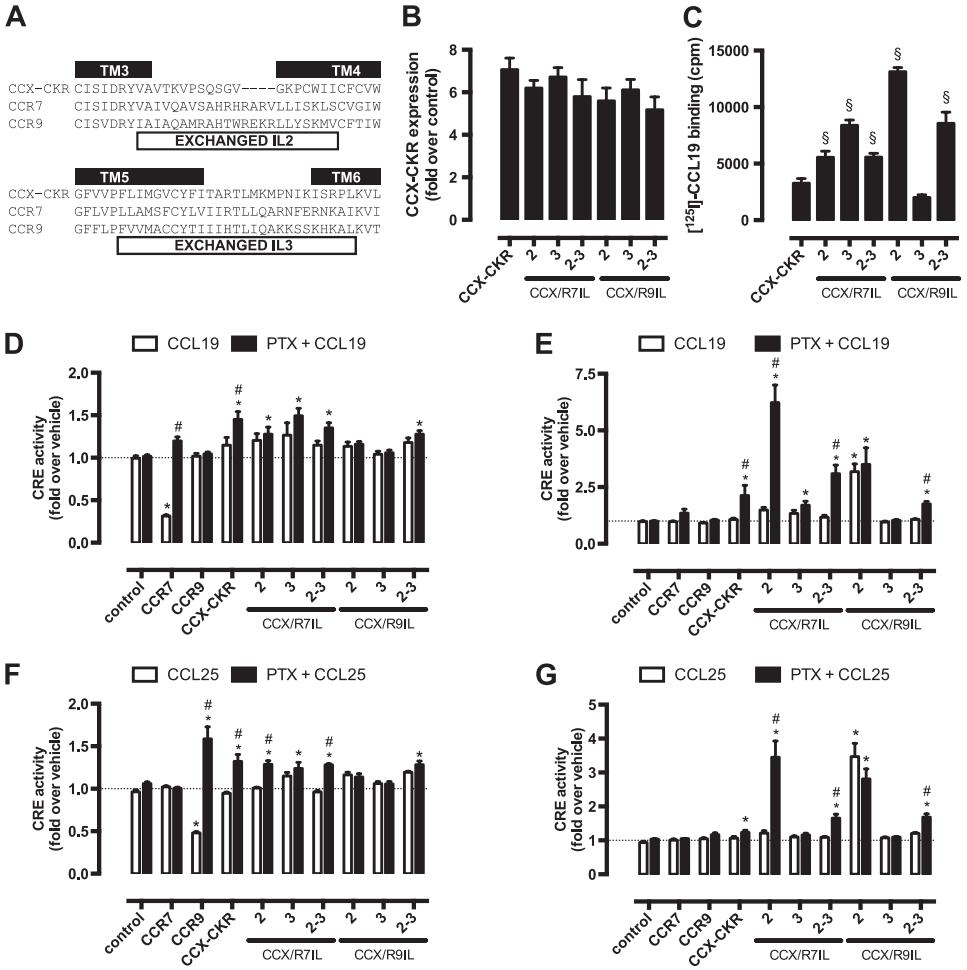

FIGURE 5. **IL2 and IL3 of functional chemokine receptors do not convey Gα_i-activating properties to CCX-CKR.** *A*, CCX-CKR, CCR7, and CCR9 amino acid sequences of TM3-IL2-TM4 and TM5-IL3-TM6 are aligned on the basis of highly conserved residues. The IL2 and IL3 sequences that have been exchanged in the CCX-CKR chimeras are indicated with *white boxes*. HEK293T cells were co-transfected with a CRE-driven reporter gene and CCX-CKR, CCX/R7IL2, CCX/R7IL3, CCX/R7IL2IL3, CCX/R9IL2, CCX/R9IL3, or CCX/R9IL2IL3 as indicated. *B*, cell surface expression was measured by ELISA. *C*, ^{125}I-CCL19 binding was performed on intact cells. Cells were pre-treated with PTX (100 ng/ml) overnight (*filled bars*). Cells were treated with vehicle, 100 nM CCL19 (*D* and *E*), or 100 nM CCL25 (*F* and *G*) for 5 h in the presence (*D* and *F*) or absemce (*E* and *G*) of 1 μM FSK. Statistical comparisons were performed using one-way analysis of variance followed by the Bonferroni test. Significant difference in cell surface expression and ^{125}I-CCL19 binding as compared with wild type CCX-CKR is indicated by §. *B* and *C*, significant difference ($p < 0.05$) in CRE activity between vehicle and corresponding chemokine-treated cells is indicated by *, whereas # indicates significant difference in chemokine-induced CRE activity between cells pretreated with or without PTX (*D*–*G*). Data are shown as averages ± S.E. of fold over vehicle data from 4 independent experiments performed in duplicate (*B*–*E*) or 2 independent experiments performed in triplicate (*F* and *G*).

expected CCL25 activated CCR9 but not CCR7, resulting in an inhibition of forskolin-induced CRE activity (Fig. 5*F*). Surprisingly, however, PTX pretreatment significantly increased CCR9-mediated CRE activity upon CCL25 stimulation in a forskolin-dependent manner (Fig. 5*F*).

G_i Proteins Impair CCX-CKR Signaling to CRE—The apparent ability of wild type CCX-CKR to stimulate CRE-mediated luciferase activity in response to CCL19 upon PTX pre-treatment, prompted us to focus on wild type CCX-CKR signaling to CRE in more detail. First, concentration-response curves of CCL19, CCL21, and CCL25 were measured in the absence and presence of PTX (100 ng/ml) and/or FSK (1 μM). In the absence of PTX pre-treatment, these chemokines did not affect CRE activity in the absence (control) or presence of FSK, when tested at concentrations up to 316 nM (Fig. 7, *A*–*C*). Pre-treatment overnight with PTX resulted in an increased CRE activity upon stimulation with >100 nM CCL19 or >316 nM CCL25 (Fig. 7, *A*–*C*). Interestingly, pre-treatment with PTX and chemokine stimulation in the presence of FSK showed that PTX and FSK synergistically increased CRE activity upon stimulation with CCL19, CCL21, or CCL25 as compared with vehicle-stimulated cells (Fig. 7, *A*–*C*). Moreover, this co-treatment with PTX and FSK significantly increased cAMP levels in HEK293T cells co-expressing CCX-CKR and a BRET-based cAMP biosensor upon stimulation with 100 nM CCL19 as compared with cells that were not pre-treated with PTX and/or stimulated with vehicle (Fig. 7*D*). Binding of cAMP to the EPAC domain of the biosensor results in a decrease of intramolecular BRET (23, 24).

Co-transfection of PTX-insensitive Gα_{i1}-C351I, Gα_{i2}-C352I, or Gα_{i3}-C351I mutants (29) in CCX-CKR-expressing cells abolished the CCL19-induced increase in CRE activity upon PTX pre-treatment (Fig. 7*E*), which suggests that interaction of G_i proteins with CCX-CKR impairs signaling of this receptor to CRE. Co-expression of the PTX-resistant G_i proteins did not affect CCX-CKR surface levels or limit expression of the luciferase reporter gene in response to 10 μM FSK (data

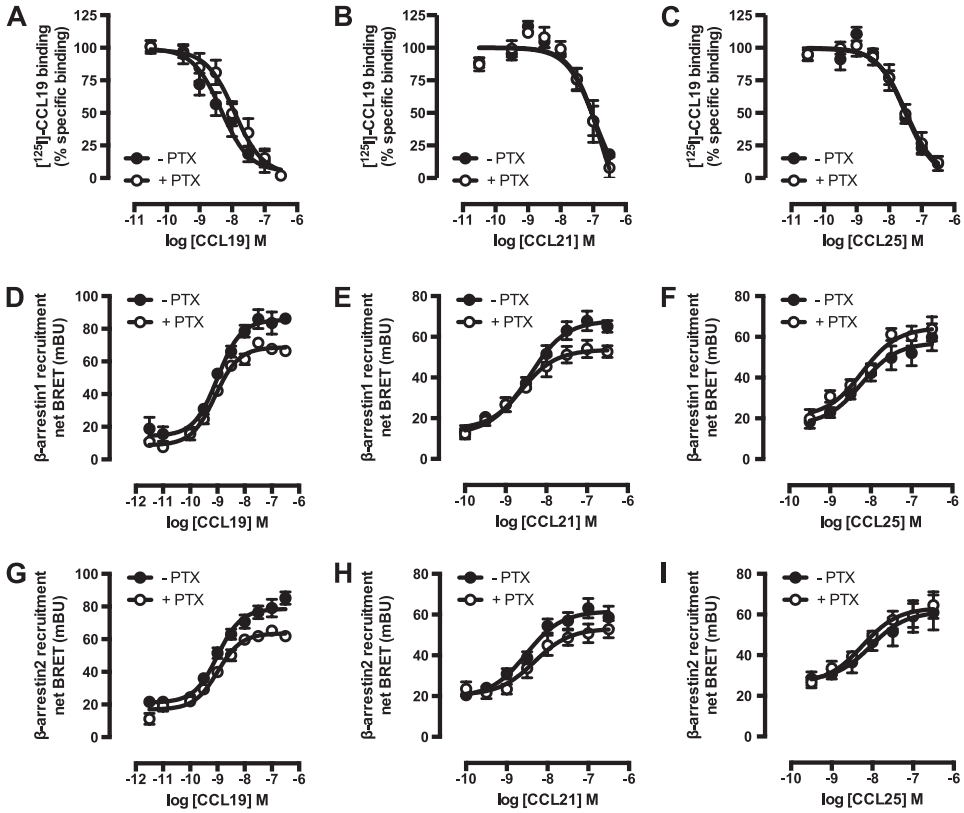

FIGURE 6. **CCX-CKR chemokine binding affinities are not dependent on $G\alpha_i$ proteins.** ^{125}I-CCL19 displacement curves were performed for CCL19 (*A*), CCL21 (*B*), and CCL25 (*C*) in the absence (*empty symbols*) and presence (*filled symbols*) of 100 ng/ml of PTX in HEK293T cells transiently transfected with CCX-CKR. β-Arrestin1 (*D–F*) and β-arrestin2 (*G–I*) recruitment induced by CCL19 (*D* and *G*), CCL21 (*E* and *H*), and CCL25 (*F* and *I*) were determined using a BRET-based assay in HEK293T cells transiently co-transfected with CCX-CKR-Rluc and β-arrestin-EYFP without (*empty symbols*) and with (*filled symbols*) PTX (100 ng/ml) pretreatment. Data are shown as averages ± S.E. of normalized specific binding of two independent experiments performed in duplicate.

not shown). Functional expression of the $G\alpha_{i1}$-C351I, $G\alpha_{i2}$-C352I, or $G\alpha_{i3}$-C351I mutants was confirmed by the inability of PTX to inhibit FSK-induced CRE activity by CCR7 upon stimulation with CCL19 (Fig. 7*E*).

CCX-CKR-mediated CRE Activation Requires an Intact DRY Motif—The conserved DRY motif of GPCRs at the border of transmembrane domain 3 and IL2 is known to be essential for controlling G protein activation, and mutation of $Arg^{3.50}$ to alanine in this motif generally results in a receptor that is unable to activate G proteins (30). Wild type CCX-CKR and CCX/R3.50A were expressed at similar levels (*t* test $p > 0.05$) at the cell surface (Fig. 8*A*). Similar to wild type CCX-CKR (Fig. 6*A*) and had comparable affinities for CCL19 with or without PTX pre-treatment (Fig. 8*B*). In contrast to wild type CCX-CKR, CCX/R3.50A was unable to activate CRE upon CCL19 stimulation in cells pre-treated with PTX (Fig. 8*C*), which supports the hypothesis that activation of CRE by wild type CCX-CKR is G protein-dependent.

PTX Pre-treatment Did Not Unmask CRE Activation by CXCR7—Several studies indicated that CXCR7 is seen as a decoy receptor due to its incapability to induce G protein signaling (18, 31). On the other hand, CXCR7 signals to ERK1/2 and Akt in a β-arrestin-biased manner upon stimulation with CXCL11/ITAC or CXCL12/SDF1α (18, 31). CXCR7-expressing HEK293T cells were pre-treated overnight with PTX to evaluate whether G_i proteins might hamper CXCR7-induced G protein signaling via a similar mechanism as observed for CCX-CKR. The CXCR7 chemokines CXCL11 and CXCL12 (100 nM) were not able to increase FSK-induced CRE activity in the absence or presence of PTX in cells transfected with CXCR7 (Fig. 9). CXCL12 decreased FSK-induced CRE activity in mock and CXCR7-expressing HEK293T cells that were not pre-treated with PTX, by interacting with the chemokine receptor CXCR4 (Fig. 9). CXCR4 is endogenously expressed on HEK293(T) cells (32).

DISCUSSION

CCX-CKR plays an important role in controlling the migration of immune and cancer cells that express chemokine receptors CCR7 and CCR9, by reducing the availability of CCL19, CCL21, and CCL25 through internalization (8, 10, 11, 15). CCX-CKR internalization was previously found to be independent of β-arrestins and clathrin-coated pits, as dominant-negative β-arrestin, Eps15 and Rab5 mutants did not impair CCL19 internalization in CCX-CKR-expressing HEK293 cells (10). In addition, CCL19 was internalized in β-arrestin1/2-null mouse embryo fibroblasts expressing CCX-CKR but not in cells expressing CCR7 (10). On the other hand, dominant-negative caveolin isoforms and cholesterol depletion diminished CCL19 sequestering by CCX-CKR, which indicated that CCX-CKR is internalized via caveolae (10). However, inspection of the intracellular C-terminal tail of CCX-CKR reveals the presence of multiple serine and threonine residues that might function as substrate for GPCR kinases and promote interaction with β-ar-

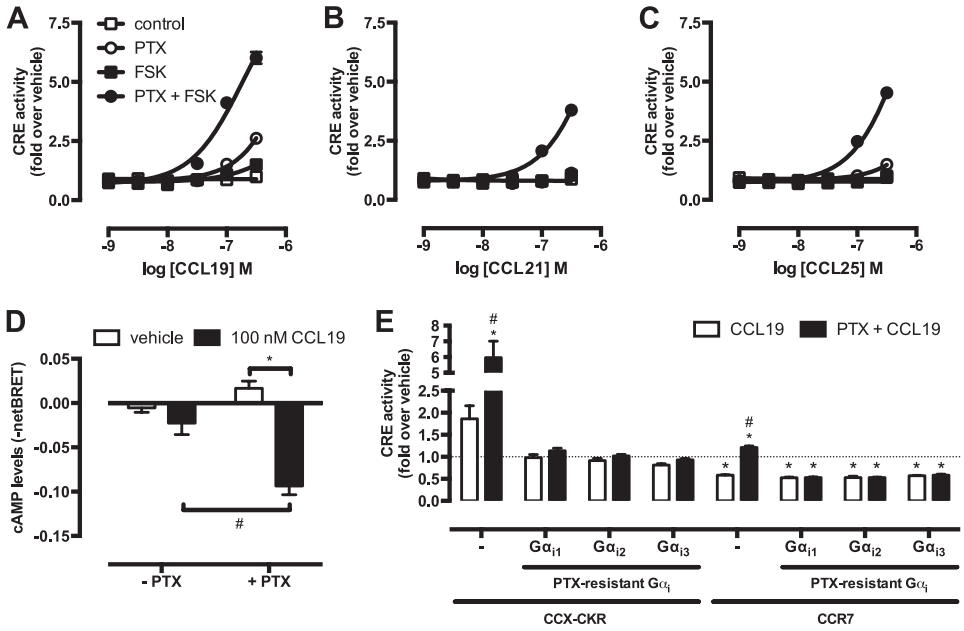

FIGURE 7. **PTX potentiates ligand-induced CRE activation mediated by CCX-CKR.** *A–C*, HEK293T cells were co-transfected with a CRE-driven reporter gene and CCX-CKR. Concentration-response curves of CCL19 (*A*), CCL21 (*B*), and CCL25 (*C*) were obtained in the absence of PTX and FSK (□), in the presence of 1 μM FSK (■), in the presence of 100 ng/ml of PTX (○), or the presence of both PTX and FSK (●). *D*, HEK293T cells were transiently transfected with the CCX-CKR-coding plasmid along with a plasmid encoding the CAMYEL cAMP biosensor. Cells were pre-treated or not with 100 ng/ml of PTX overnight. Cells were stimulated with 100 nM CCL19 in the presence of 1 μM FSK for 10 min prior to measurement of the intramolecular BRET signal. Elevation of cAMP levels is detected as decreased BRET ratio. Data are shown as averages ± S.E. of normalized and baseline corrected BRET ratios from three independent experiments performed in duplicate. *E*, HEK293T cells were co-transfected with a CRE-driven reporter gene, CCX-CKR, or CCR7 and the PTX-insensitive mutants of $G\alpha_i$ subunit $G\alpha_{i1}$/C351I, $G\alpha_{i2}$/C352I, and $G\alpha_{i3}$/C351I as indicated. Cells were pre-treated (*black bars*) or not (*empty bars*) with 100 ng/ml of PTX overnight. Cells were incubated with vehicle or 100 nM CCL19 in the presence of 1 μM FSK for 6 to 8 h. Statistical comparisons to identify significant differences between vehicle and chemokine-stimulated cells (*) as well as between control and PTX-pretreated cells (#) were performed using one-way analysis of variance followed by the Bonferroni test. *p* value < 0.05 indicate significant difference. Graphs (*A-C* and *E*) show averages ± S.E. of fold over vehicle data from three to six independent experiments performed in duplicate.

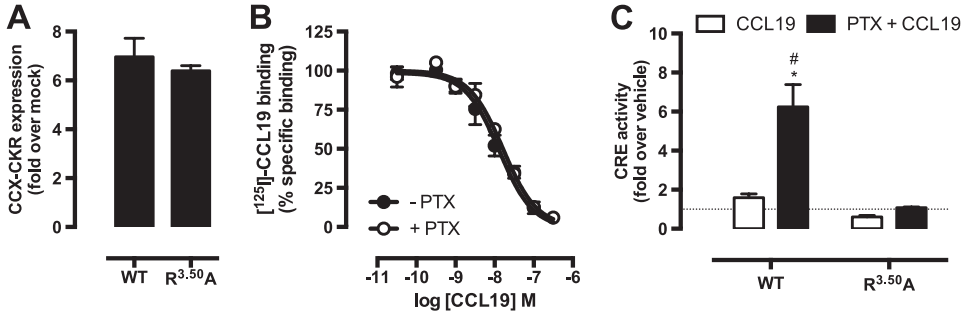

FIGURE 8. **Potentiation of CCX-CKR-mediated CRE activation is G protein-dependent.** *A*, cell surface expression of wild type CCX-CKR and the DRY mutant CCX/R3.50A in the reporter gene assay was determined using ELISA with anti-CCX-CKR antibody. Graph shows averages ± S.E. of fold over mock data from two independent experiments performed in duplicate. *B*, ^{125}I-CCL19 displacement curves with CCL19 were obtained in the absence (*empty symbols*) or presence (*filled symbols*) of 100 ng/ml of PTX in HEK293T cells transfected with CCX/R3.50A. Data are shown as averages ± S.E. of normalized specific binding of one independent experiment performed in duplicate. *C*, HEK293T cells were co-transfected with a CRE-driven reporter gene and wild type CCX-CKR or CCX/R3.50A as indicated. Cells were pre-treated with 100 ng/ml of PTX (*empty* and *black bars*) overnight. Cells were incubated with vehicle (*empty bars*) or 100 nM CCL19 (*filled bars*) in the presence of 1 μM FSK for 5 h. Statistical comparisons to identify significant differences between vehicle and chemokine-stimulated cells (*) as well as between control and PTX-pretreated cells (#) were performed using one-way analysis of variance followed by the Bonferroni test. *p* value < 0.05 indicate significant difference. Graph show averages ± S.E. of fold over vehicle data from two independent experiments performed in duplicate.

restins upon phosphorylation (33). In this study, we demonstrate for the first time that stimulation of CCX-CKR with CCL19, CCL21, and CCL25 indeed induced β-arrestin2-GFP translocation. CCX-CKR did not translocate β-arrestin2-GFP in the absence of chemokines, which is in contrast to the constitutively phosphorylated chemokine decoy receptor D6 (21). Moreover, fluorescently labeled CCL19 co-localized in the same intracellular vesicles as β-arrestin2-GFP, suggesting recruitment of β-arrestin to CCL19-bound CCX-CKR. Enzyme fragment complementation and BRET, which are two different close proximity-based approaches, then demonstrated actual recruitment of β-arrestin to CCX-CKR in response to chemokines. The recruitment of β-arrestin to CCX-CKR and co-localization with internalized CCL19 suggests that a possible involvement of β-arrestins in CCX-CKR endocytosis cannot be excluded. The occurrence of parallel internalization pathways for one receptor is not unprecedented. For instance, the dopamine D_1 receptor internalizes through both caveolae and clathrin-coated pits (34, 35). Interestingly, inhibition of clathrin-coated pit-dependent endocytosis by various methods did

not affect D_1 receptor internalization, suggesting that β-arrestin and clathrin-coated pits might not be the dominant pathway for this receptor (34).

Besides functioning as an interaction site for proteins of the endocytotic machinery, GPCR-bound β-arrestin can also assemble specific signaling scaffolds, such as, for example, β-arrestin2/ERK/Raf/MEK and Akt/β-arrestin2/PP2A (36, 37). CCX-CKR was, however, unable to activate downstream signaling to ERK1/2 and Akt upon stimulation with CCL19, whereas CCL19 activates ERK1/2 in a β-arrestin2-dependent manner via CCR7 (38). Importantly, β-arrestin can activate numerous other kinases as well as phosphatases in addition to ERK1/2 and Akt (39) and the activation of these additional signal effectors through CCX-CKR remains to be investigated, preferably in physiologically relevant assay systems.

Previous studies showed that CCX-CKR is unable to induce G protein-dependent intracellular Ca^{2+} mobilization (7, 14). In line with these observations and in contrast to CCR7 and CCR9, CCX-CKR was unable to modulate intracellular cAMP and inositol phosphate levels upon stimulation with 100 nM CCL19, CCL21, and CCL25. Nevertheless, analysis of the CCX-CKR amino acid sequence reveals the conservation of typical GPCR signaling motifs at the bottom of TM helix 3 (*i.e.* DRY) and TM7 helix 8 (*i.e.* NP*XXY*$(X)_7$F) (40–42), as well as a reasonable sequence identity with CCR7 and CCR9 in the TM helices that flank intracellular loops 2 and 3 (Fig. 6*A*). Interestingly, substitution of CCX-CKR IL2 and/or IL3 with corresponding CCR7 and CCR9 sequences conferred a small but consistent CRE stimulatory activity to CCX-CKR mutants in response to chemokines, rather than the anticipated G_i-mediated decrease in CRE signaling. Preventing G_i protein interaction with GPCRs by pre-treating the cells with PTX resulted in a potentiation of this signaling by the CCX-CKR mutants. In the absence of forskolin, PTX treatment resulted in a significant chemokine-induced CRE activation by CCX/R7IL2, whereas CCX/R9IL2 activated CRE both in the absence and presence of PTX. These data for the two CCX-CKR chimeras suggest that the IL2 of CCX-CKR decreases the propensity to interact with G proteins.

Moreover, this PTX pre-treatment unmasked signaling by wild type CCX-CKR, resulting in a significant increase in CRE activity in response to CCL19, CCL21, and CCL25. The chemokine concentration-response curves did not allow proper determination of potency and efficacy. However, CCL19 seemed slightly more potent to activate CRE than CCL21 and CCL25, which corresponds to their rank order of CCX-CKR affinities and the β-arrestin recruitment potencies in the different assay formats (Table 1). Interestingly, all ligands are ~30–100-fold less potent to stimulate CRE activity in comparison to recruiting β-arrestins, which might suggest that β-arrestin is not involved in CRE activation in PTX-treated CCX-CKR-expressing cells by interacting with the transcription factor cAMP-response element-binding protein and the histone acetyltransferase p300 as previously observed for the δ-opioid receptor (43). Moreover, the absence of CCL19-induced ERK1/2 phosphorylation in CCX-CKR-expressing cells indicates that CRE activation is also not induced via a β-arrestin- and ERK1/2-dependent pathway, which has been recently described in tracheal epithelial cells (44).

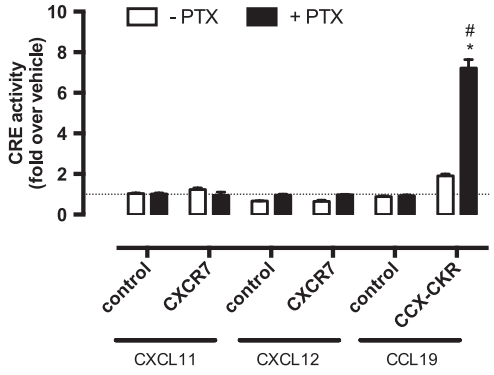

FIGURE 9. **CXCR7 does not mediate CRE activation.** HEK293T cells were co-transfected with a CRE-driven reporter gene and empty vector (−), CXCR7, or CCX-CKR as indicated. Cells were pre-treated (*black bars*) or not (*empty bars*) with 100 ng/ml of PTX overnight. Cells were incubated with vehicle, CXCL11, CXCL12, or CCL19 (100 nM chemokine) as indicated in the presence of 1 μM FSK. Data are shown as averages ± S.E. of fold over vehicle data from two independent experiments performed in duplicate. Statistical comparisons to identify significant differences between vehicle and chemokine-stimulated cells (*) as well as between control and PTX-pretreated cells (#) were performed using one-way analysis of variance followed by the Bonferroni test. p value < 0.05 indicate significant difference.

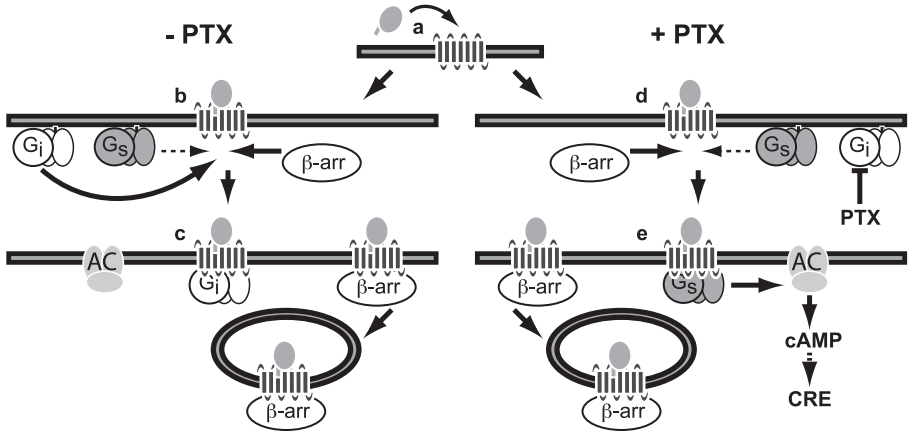

FIGURE 10. **Proposed model of CCX-CKR interaction with β-arrestins and G proteins.** Chemokine binding to CCX-CKR (*a*) recruits G_i proteins and β-arrestin (*β-arr*) with high affinity (*b*), consequently hindering the low affinity interaction between CCX-CKR and G_s proteins. Inactive G_i protein may stay bound to CCX-CKR, whereas the chemokine-bound CCX-CKR internalizes with β-arrestin (*c*). Inhibition of G_i coupling to CCX-CKR by PTX pre-treatment did not affect β-arrestin recruitment but allows G_s to interact with CCX-CKR (*d*), which results in stimulation of adenylyl cyclase (*AC*) and CRE activity (*e*).

The recent crystal structure of the β2-adrenoreceptor in complex with the $G\alpha_s$ protein showed that the conserved $Arg^{3.50}$ in the DRY motif interacts directly with the G protein (42), which was earlier observed as well in the structure of opsin in complex with a C-terminal peptide of the Gα protein (45). Ala substitution of $Arg^{3.50}$ in CCX-CKR completely abolished CCL19-induced CRE activation in PTX-treated cells, suggesting that the interaction of PTX-insensitive G proteins with CCX-CKR is crucial to signal to CRE. Besides G_s proteins, G_q proteins have also been shown to stimulate several adenylyl cyclase subtypes via their βγ-subunits (46, 47). The fact that CCX-CKR-mediated CRE activation is only observed after disabling G_i proteins to interact with the receptor suggests that G_i proteins might impair the interaction of PTX-insensitive G proteins to couple to CCX-CKR upon chemokine stimulation. The atypical chemokine receptor CXCR7 signals exclusively through β-arrestins (18, 31). Interestingly, however, BRET assays showed that CXCR7 interacts constitutively with G_i proteins without activating them (48). A similar scenario of constitutive or chemokine-induced interaction of inactive G_i proteins with CCX-CKR is hypothesized to maintain this decoy receptor "silenced" for typical chemokine receptor-induced G protein signaling by impeding subsequent and apparently less favorable coupling of PTX-insensitive G proteins to this receptor (Fig. 10). On the other hand, pre-treatment of CXCR7-expressing cells with PTX did not unmask CRE activation in response to CXCL11 and CXCL12, suggesting that G_i-mediated silencing of CCX-CKR-induced CRE activation is at least specific for this receptor and not the consequence of other cellular changes. Detection of G protein interactions with CCX-CKR using BRET-based methods might unravel the identity and dynamics of G protein subtypes that are recruited to the receptor.

In conclusion, the atypical chemokine receptor CCX-CKR is capable of increasing cAMP levels and CRE activity in response to chemokine stimulation, however, PTX-sensitive G proteins normally prevent this signaling. On the other hand, the chemokine-induced recruitment of β-arrestins to CCX-CKR might open avenues to activate yet to be identified G protein-independent signaling pathways.

Acknowledgments—We thank Winfried Mulder (MSD), Marloes van der Zwam and Dr. Biber (University of Groningen, The Netherlands), and Dr. Chiba (Tokyo University of Science, Japan) for providing reagents.

REFERENCES

1. Scholten, D. J., Canals, M., Maussang, D., Roumen, L., Smit, M. J., Wijtmans, M., de Graaf, C., Vischer, H. F., and Leurs, R. (2012) Pharmacological modulation of chemokine receptor function. *Br. J. Pharmacol.* **165,** 1617–1643
2. O'Hayre, M., Salanga, C. L., Handel, T. M., and Allen, S. J. (2008) Chemokines and cancer. Migration, intracellular signalling and intercellular communication in the microenvironment. *Biochem. J.* **409,** 635–649
3. Ulvmar, M. H., Hub, E., and Rot, A. (2011) Atypical chemokine receptors. *Exp. Cell Res.* **317,** 556–568
4. Gosling, J., Dairaghi, D. J., Wang, Y., Hanley, M., Talbot, D., Miao, Z., and Schall, T. J. (2000) Cutting edge. Identification of a novel chemokine receptor that binds dendritic cell- and T cell-active chemokines including ELC, SLC, and TECK. *J. Immunol.* **164,** 2851–2856
5. Förster, R., Davalos-Misslitz, A. C., and Rot, A. (2008) CCR7 and its ligands. Balancing immunity and tolerance. *Nat. Rev. Immunol.* **8,** 362–371
6. Pabst, O., Ohl, L., Wendland, M., Wurbel, M. A., Kremmer, E., Malissen, B., and Förster, R. (2004) Chemokine receptor CCR9 contributes to the localization of plasma cells to the small intestine. *J. Exp. Med.* **199,** 411–416
7. Heinzel, K., Benz, C., and Bleul, C. C. (2007) A silent chemokine receptor regulates steady-state leukocyte homing *in vivo*. *Proc. Natl. Acad. Sci. U.S.A.* **104,** 8421–8426
8. Comerford, I., Nibbs, R. J., Litchfield, W., Bunting, M., Harata-Lee, Y., Haylock-Jacobs, S., Forrow, S., Korner, H., and McColl, S. R. (2010) The atypical chemokine receptor CCX-CKR scavenges homeostatic chemokines in circulation and tissues and suppresses Th17 responses. *Blood* **116,** 4130–4140
9. Lazennec, G., and Richmond, A. (2010) Chemokines and chemokine receptors. New insights into cancer-related inflammation. *Trends Mol. Med.* **16,** 133–144
10. Comerford, I., Milasta, S., Morrow, V., Milligan, G., and Nibbs, R. (2006) The chemokine receptor CCX-CKR mediates effective scavenging of CCL19 *in vitro*. *Eur. J. Immunol.* **36,** 1904–1916
11. Feng, L. Y., Ou, Z. L., Wu, F. Y., Shen, Z. Z., and Shao, Z. M. (2009) Involvement of a novel chemokine decoy receptor CCX-CKR in breast cancer growth, metastasis and patient survival. *Clin. Cancer Res.* **15,** 2962–2970
12. Haraldsen, G., and Rot, A. (2006) Coy decoy with a new ploy. Interceptor controls the levels of homeostatic chemokines. *Eur. J. Immunol.* **36,** 1659–1661
13. Khoja, H., Wang, G., Ng, C. T., Tucker, J., Brown, T., and Shyamala, V. (2000) Cloning of CCRL1, an orphan seven transmembrane receptor related to chemokine receptors, expressed abundantly in the heart. *Gene* **246,** 229–238
14. Townson, J. R., and Nibbs, R. J. (2002) Characterization of mouse CCX-CKR, a receptor for the lymphocyte-attracting chemokines TECK/mCCL25, SLC/mCCL21 and MIP-3β/mCCL19. Comparison to human CCX-CKR. *Eur. J. Immunol.* **32,** 1230–1241
15. Kriegova, E., Tsyrulnyk, A., Arakelyan, A., Mrazek, F., Ordeltova, M., Petzmann, S., Zatloukal, J., Kolek, V., du Bois, R. M., Popper, H., and Petrek, M. (2006) Expression of CCX CKR in pulmonary sarcoidosis. *Inflamm. Res.* **55,** 441–445
16. Rode, I., and Boehm, T. (2012) Regenerative capacity of adult cortical thymic epithelial cells. *Proc. Natl. Acad. Sci. U.S.A.* **109,** 3463–3468
17. Rajagopal, S., Rajagopal, K., and Lefkowitz, R. J. (2010) Teaching old receptors new tricks. Biasing seven-transmembrane receptors. *Nat. Rev. Drug Discov.* **9,** 373–386
18. Rajagopal, S., Kim, J., Ahn, S., Craig, S., Lam, C. M., Gerard, N. P., Gerard, C., and Lefkowitz, R. J. (2010) β-Arrestin- but not G protein-mediated signaling by the "decoy" receptor CXCR7. *Proc. Natl. Acad. Sci. U.S.A.* **107,** 628–632
19. Luker, K. E., Gupta, M., and Luker, G. D. (2009) Imaging chemokine receptor dimerization with firefly luciferase complementation. *FASEB J.* **23,** 823–834
20. Galliera, E., Jala, V. R., Trent, J. O., Bonecchi, R., Signorelli, P., Lefkowitz, R. J., Mantovani, A., Locati, M., and Haribabu, B. (2004) β-Arrestin-dependent constitutive internalization of the human chemokine decoy receptor D6. *J. Biol. Chem.* **279,** 25590–25597
21. McCulloch, C. V., Morrow, V., Milasta, S., Comerford, I., Milligan, G., Graham, G. J., Isaacs, N. W., and Nibbs, R. J. (2008) Multiple roles for the C-terminal tail of the chemokine scavenger D6. *J. Biol. Chem.* **283,** 7972–7982
22. Vischer, H. F., Nijmeijer, S., Smit, M. J., and Leurs, R. (2008) Viral hijacking of human receptors through heterodimerization. *Biochem. Biophys. Res. Commun.* **377,** 93–97
23. Scholten, D. J., Canals, M., Wijtmans, M., de Munnik, S., Nguyen, P., Verzijl, D., de Esch, I. J., Vischer, H. F., Smit, M. J., and Leurs, R. (2012) Pharmacological characterization of a small-molecule agonist for the chemokine receptor CXCR3. *Br. J. Pharmacol.* **166,** 898–911
24. Jiang, L. I., Collins, J., Davis, R., Lin, K. M., DeCamp, D., Roach, T., Hsueh, R., Rebres, R. A., Ross, E. M., Taussig, R., Fraser, I., and Sternweis, P. C.

(2007) Use of a cAMP BRET sensor to characterize a novel regulation of cAMP by the sphingosine 1-phosphate/G_{13} pathway. *J. Biol. Chem.* **282,** 10576–10584
25. Van Lith, L. H., Oosterom, J., Van Elsas, A., and Zaman, G. J. (2009) C5a-stimulated recruitment of β-arrestin2 to the nonsignaling 7-transmembrane decoy receptor C5L2. *J. Biomol. Screen.* **14,** 1067–1075
26. Nijmeijer, S., Leurs, R., Smit, M. J., and Vischer, H. F. (2010) The Epstein-Barr virus-encoded G protein-coupled receptor BILF1 hetero-oligomerizes with human CXCR4, scavenges $G\alpha_i$ proteins, and constitutively impairs CXCR4 functioning. *J. Biol. Chem.* **285,** 29632–29641
27. van Der Lee, M. M., Bras, M., van Koppen, C. J., and Zaman, G. J. (2008) β-Arrestin recruitment assay for the identification of agonists of the sphingosine 1-phosphate receptor EDG1. *J. Biomol. Screen.* **13,** 986–998
28. Blomenröhr, M., Heding, A., Sellar, R., Leurs, R., Bogerd, J., Eidne, K. A., and Willars, G. B. (1999) Pivotal role for the cytoplasmic carboxyl-terminal tail of a nonmammalian gonadotropin-releasing hormone receptor in cell surface expression, ligand binding, and receptor phosphorylation and internalization. *Mol. Pharmacol.* **56,** 1229–1237
29. Bahia, D. S., Wise, A., Fanelli, F., Lee, M., Rees, S., and Milligan, G. (1998) Hydrophobicity of residue 351 of the G protein Gi1α determines the extent of activation by the α2A-adrenoceptor. *Biochemistry* **37,** 11555–11562
30. Rovati, G. E., Capra, V., and Neubig, R. R. (2007) The highly conserved DRY motif of class A G protein-coupled receptors. Beyond the ground state. *Mol. Pharmacol.* **71,** 959–964
31. Kumar, R., Tripathi, V., Ahmad, M., Nath, N., Mir, R. A., Chauhan, S. S., and Luthra, K. (2012) CXCR7 mediated Giα independent activation of ERK and Akt promotes cell survival and chemotaxis in T cells. *Cell. Immunol.* **272,** 230–241
32. Atwood, B. K., Lopez, J., Wager-Miller, J., Mackie, K., and Straiker, A. (2011) Expression of G protein-coupled receptors and related proteins in HEK293, AtT20, BV2, and N18 cell lines as revealed by microarray analysis. *BMC Genomics* **12,** 14
33. Liggett, S. B. (2011) Phosphorylation barcoding as a mechanism of directing GPCR signaling. *Sci. Signal.* **4,** pe36
34. Kong, M. M., Hasbi, A., Mattocks, M., Fan, T., O'Dowd, B. F., and George, S. R. (2007) Regulation of D1 dopamine receptor trafficking and signaling by caveolin-1. *Mol. Pharmacol.* **72,** 1157–1170
35. Vickery, R. G., and von Zastrow, M. (1999) Distinct dynamin-dependent and -independent mechanisms target structurally homologous dopamine receptors to different endocytic membranes. *J. Cell Biol.* **144,** 31–43
36. Shenoy, S. K., and Lefkowitz, R. J. (2011) β-Arrestin-mediated receptor trafficking and signal transduction. *Trends Pharmacol. Sci.* **32,** 521–533
37. DeFea, K. A. (2011) β-arrestins as regulators of signal termination and transduction. How do they determine what to scaffold? *Cell. Signal.* **23,** 621–629
38. Zidar, D. A., Violin, J. D., Whalen, E. J., and Lefkowitz, R. J. (2009) Selective engagement of G protein-coupled receptor kinases (GRKs) encodes distinct functions of biased ligands. *Proc. Natl. Acad. Sci. U.S.A.* **106,** 9649–9654
39. Xiao, K., Sun, J., Kim, J., Rajagopal, S., Zhai, B., Villén, J., Haas, W., Kovacs, J. J., Shukla, A. K., Hara, M. R., Hernandez, M., Lachmann, A., Zhao, S., Lin, Y., Cheng, Y., Mizuno, K., Ma'ayan, A., Gygi, S. P., and Lefkowitz, R. J. (2010) Global phosphorylation analysis of β-arrestin-mediated signaling downstream of a seven transmembrane receptor (7TMR). *Proc. Natl. Acad. Sci. U.S.A.* **107,** 15299–15304
40. Rosenbaum, D. M., Rasmussen, S. G., and Kobilka, B. K. (2009) The structure and function of G-protein-coupled receptors. *Nature* **459,** 356–363
41. Nygaard, R., Frimurer, T. M., Holst, B., Rosenkilde, M. M., and Schwartz, T. W. (2009) Ligand binding and micro-switches in 7TM receptor structures. *Trends Pharmacol. Sci.* **30,** 249–259
42. Rasmussen, S. G., DeVree, B. T., Zou, Y., Kruse, A. C., Chung, K. Y., Kobilka, T. S., Thian, F. S., Chae, P. S., Pardon, E., Calinski, D., Mathiesen, J. M., Shah, S. T., Lyons, J. A., Caffrey, M., Gellman, S. H., Steyaert, J., Skiniotis, G., Weis, W. I., Sunahara, R. K., and Kobilka, B. K. (2011) Crystal structure of the β2-adrenergic receptor-Gs protein complex. *Nature* **477,** 549–555
43. Kang, J., Shi, Y., Xiang, B., Qu, B., Su, W., Zhu, M., Zhang, M., Bao, G., Wang, F., Zhang, X., Yang, R., Fan, F., Chen, X., Pei, G., and Ma, L. (2005) A nuclear function of β-arrestin1 in GPCR signaling. Regulation of histone acetylation and gene transcription. *Cell* **123,** 833–847
44. Manson, M. E., Corey, D. A., Rymut, S. M., and Kelley, T. J. (2011) β-Arrestin-2 regulation of the cAMP response element binding protein. *Biochemistry* **50,** 6022–6029
45. Scheerer, P., Park, J. H., Hildebrand, P. W., Kim, Y. J., Krauss, N., Choe, H. W., Hofmann, K. P., and Ernst, O. P. (2008) Crystal structure of opsin in its G-protein-interacting conformation. *Nature* **455,** 497–502
46. Wettschureck, N., and Offermanns, S. (2005) Mammalian G proteins and their cell type-specific functions. *Physiol. Rev.* **85,** 1159–1204
47. Maruko, T., Nakahara, T., Sakamoto, K., Saito, M., Sugimoto, N., Takuwa, Y., and Ishii, K. (2005) Involvement of the βγ subunits of G proteins in the cAMP response induced by stimulation of the histamine H1 receptor. *Naunyn-Schmiedebergs Arch. Pharmacol.* **372,** 153–159
48. Levoye, A., Balabanian, K., Baleux, F., Bachelerie, F., and Lagane, B. (2009) CXCR7 heterodimerizes with CXCR4 and regulates CXCL12-mediated G protein signaling. *Blood* **113,** 6085–6093